

Convergence behavior of the MITC3+ triangular shell element

*Youngyu Lee¹⁾ and Phill-Seung Lee²⁾

¹⁾ Agency for Defense Development, Daejeon 305-600, Korea

²⁾ Department of Mechanical Engineering, KAIST, Daejeon 305-701, Korea

¹⁾ pointer423@gmail.com

ABSTRACT

In this study, we present the convergence behavior of the MITC3+ triangular shell element, which has been recently developed (Lee et. al, 2014, Jeon et. al, 2015, Lee et. al, 2015). A cubic bubble function for the rotations is used to enrich the bending displacements and the corresponding degrees of freedom can be statically condensed out on the element level. The MITC (Mixed Interpolation of Tensorial Components) method is employed to alleviate shear locking. The MITC3+ shell element passes all the basic tests (the patch, zero energy mode and isotropy tests). In convergence studies, excellent convergence behaviors are shown. In uniform meshes, the convergence behavior of the MITC3+ shell element is as good as that of the 4-node MITC4 shell element, which has been widely used in finite element analysis of shells. In distorted meshes, the MITC3+ shell element shows much better convergence behavior than the MITC4 shell element, particularly, in bending-dominated shell problems.

1. INTRODUCTION

The finite element method has been dominantly applied to analyze shell structures. It is important to use reliable and effective shell finite elements. There is still required to improve predictive capability of shell elements (Bathe, 1996, Chapelle and Bathe, 2011). One of important issues is to develop the effective 3-node triangular shell element, which is very useful for automatic mesh generations of complex shell structures (Lee and Bathe, 2004, Lee et. al, 2007, Lee et. al, 2012).

Recently, a new 3-node triangular shell finite element (MITC3+) was developed (Lee et. al, 2014). A cubic bubble function is used for the interpolation of the rotations to enrich the bending displacement fields. The corresponding rotation degrees of freedom can be statically condensed out on the element level. A new assumed transverse shear strain field was established with a new tying scheme to reduce shear

¹⁾ Senior Researcher

²⁾ Associate Professor

locking while satisfying the consistency and ellipticity conditions. The MITC3+ shell element passes the three basic tests (the patch, zero energy mode and isotropy tests) and shows excellent convergence behaviors in various shell problems even when highly distorted meshes are used (Lee et. al, 2014).

In this presentation, we show the convergence behavior of the MITC3+ triangular shell element. The results are compared with the 4-node MITC shell element (MITC4), which has been widely used in various commercial software.

In the following sections, we review the formulation of the MITC3+ triangular shell finite element and its performance is briefly presented. We then present conclusions.

2. The MITC3+ triangular shell finite element

The geometry interpolation of the MITC3+ shell element, shown in Fig. 1, is given by (Lee et. al, 2014)

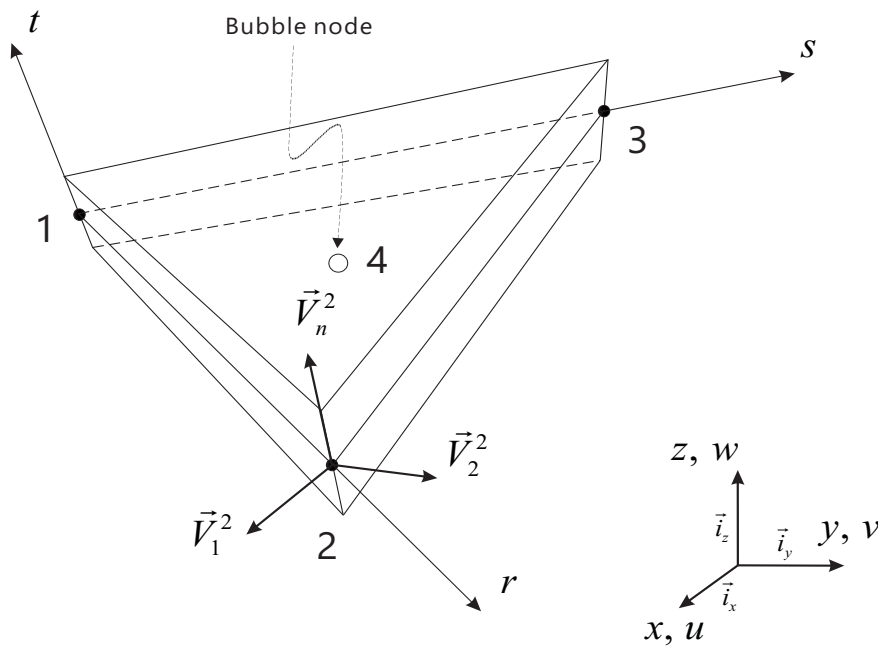


Fig. 1. Geometry of the MITC3+ shell element with an additional bubble node.

$$\bar{x}(r, s, t) = \sum_{i=1}^3 h_i(r, s) \bar{x}_i + \frac{t}{2} \sum_{i=1}^4 a_i f_i(r, s) \bar{V}_n^i \quad \text{with} \quad a_4 \bar{V}_n^4 = \frac{1}{3} (a_1 \bar{V}_n^1 + a_2 \bar{V}_n^2 + a_3 \bar{V}_n^3), \quad (1)$$

in which $h_i(r, s)$ is the two-dimensional interpolation function of the standard isoparametric procedure corresponding to node i , \bar{x}_i is the position vector of node i

in the global Cartesian coordinate system, and a_i and \vec{V}_n^i denote the shell thickness and the director vector at the node, $f_i(r, s)$ are two-dimensional interpolation functions that include the cubic bubble function f_4 corresponding to the internal node 4

$$f_1 = h_1 - \frac{1}{3}f_4, \quad f_2 = h_2 - \frac{1}{3}f_4, \quad f_3 = h_3 - \frac{1}{3}f_4, \quad f_4 = 27rs(1-r-s). \quad (2)$$

From Eq. (1), we obtain the displacement interpolation

$$\vec{u}(r, s, t) = \sum_{i=1}^3 h_i(r, s)\vec{u}_i + \frac{t}{2} \sum_{i=1}^4 a_i f_i(r, s)(-\vec{V}_2^i \alpha_i + \vec{V}_1^i \beta_i), \quad (3)$$

in which \vec{u}_i is the nodal displacement vector in the global Cartesian coordinate system, \vec{V}_1^i and \vec{V}_2^i are unit vectors orthogonal to \vec{V}_n^i and to each other, and α_i and β_i are the rotations of the director vector \vec{V}_n^i about \vec{V}_1^i and \vec{V}_2^i , respectively, at node i (α_4 and β_4 are the rotation degrees of freedom at the bubble node).

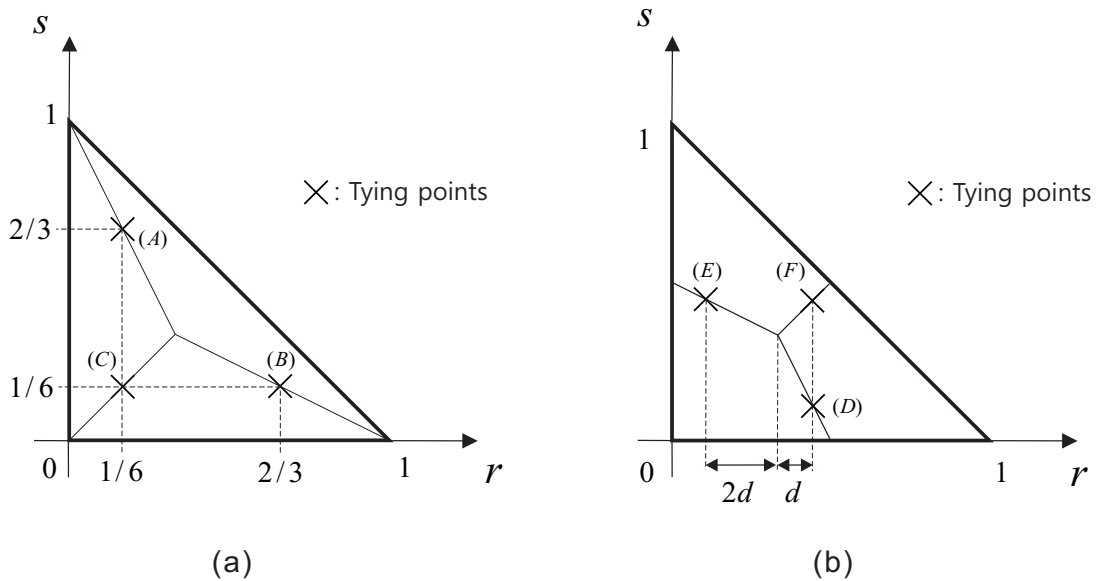


Fig. 2. Tying positions (A)-(F) used for the assumed transverse shear strain field of the MITC3+ shell finite element.

The geometry of the MITC3+ shell element is flat because the bubble node with only rotation degrees of freedom is positioned on the flat surface defined by the three corner nodes of the element. Hence, only the transverse shear strain components are assumed using the MITC method. The assumed transverse shear strain field is given by (Lee et. al, 2014)

$$\begin{aligned}\hat{e}_{rt}^{MITC3+} &= \frac{2}{3}(e_{rt}^{(B)} - \frac{1}{2}e_{st}^{(B)}) + \frac{1}{3}(e_{rt}^{(C)} + e_{st}^{(C)}) + \frac{1}{3}\hat{c}(3s-1), \\ \hat{e}_{st}^{MITC3+} &= \frac{2}{3}(e_{st}^{(A)} - \frac{1}{2}e_{rt}^{(A)}) + \frac{1}{3}(e_{rt}^{(C)} + e_{st}^{(C)}) + \frac{1}{3}\hat{c}(1-3r),\end{aligned}\quad (4)$$

in which $\hat{c} = e_{rt}^{(F)} - e_{rt}^{(D)} - e_{st}^{(F)} + e_{st}^{(E)}$ and the 6 tying points (A)-(F) with the tying distance d are shown in Fig. 2. A fixed value $d = 1/10,000$ is used in Ref. (Lee et. al, 2014).

The partly clamped hyperbolic paraboloid shell problem shown in Fig. 3 is considered (Lee and Bathe, 2002). The surface is defined as

$$Z = X^2 - Y^2; (X, Y) \in [-L/2; L/2]^2, \quad (5)$$

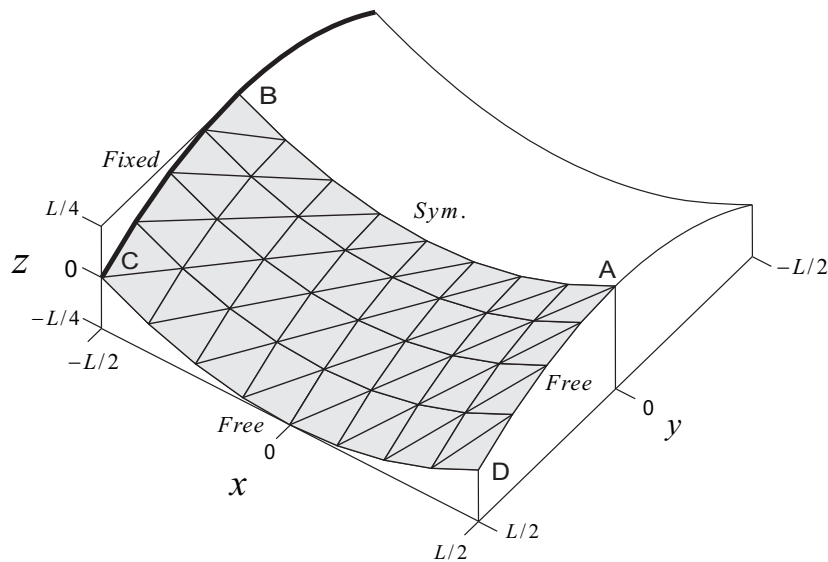


Fig. 3 Partly clamped hyperbolic paraboloid shell problem ($L=1.0$, $E = 2 \times 10^{11}$ and $\nu=0.3$).

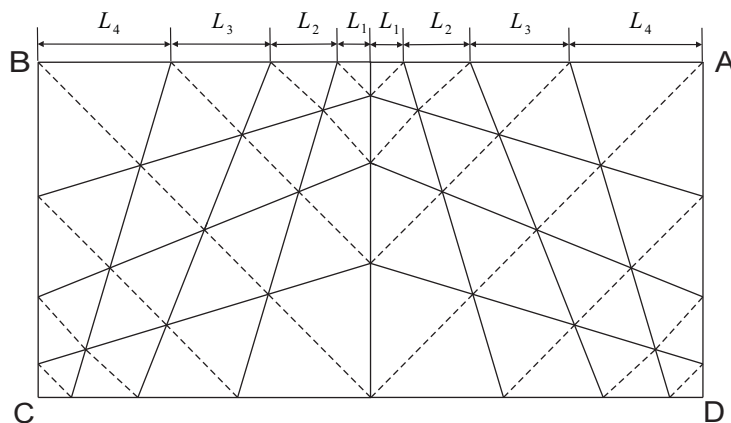


Fig. 4 Distorted mesh pattern for $N = 8$.

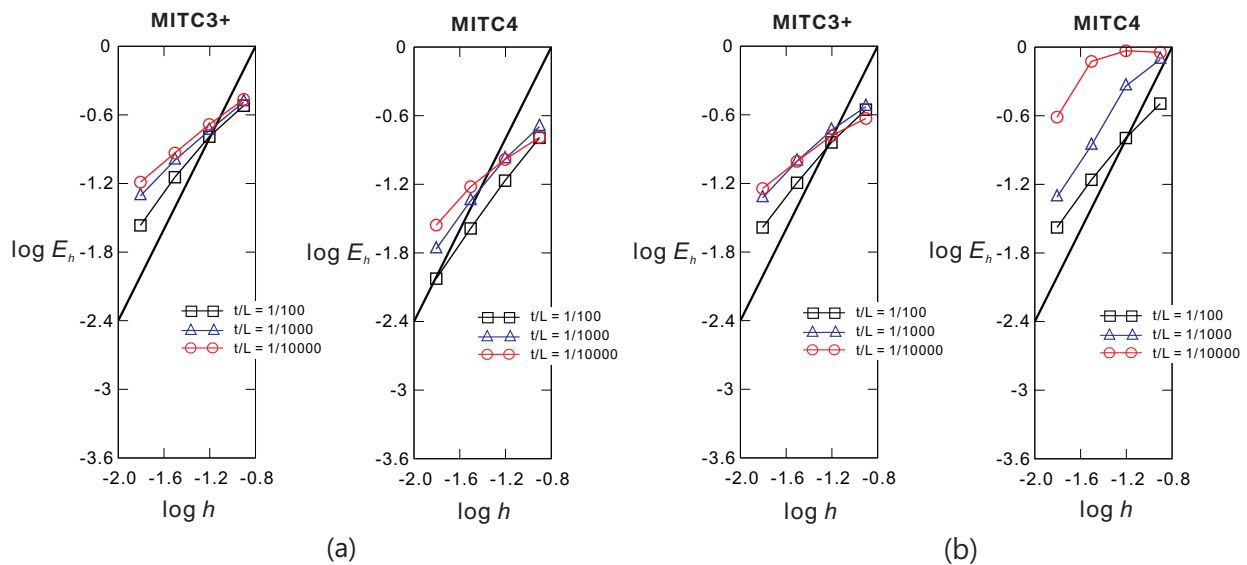


Fig. 5 Convergence curves for the partly clamped hyperbolic paraboloid shell problem. The bold line represents the optimal convergence rate. (a) Uniform mesh. (b) Distorted mesh.

and clamped along the side $X = -L/2$ and loaded by its self-weight. This shell problem is classified as a bending dominated behavior. Due to symmetry, only one half model is considered. Both the uniform mesh shown in Fig. 3 and the distorted mesh shown in Fig. 4 are considered. The s-norm is used for the convergence studies (Hiller and Bathe, 2003). Fig. 5 presents the convergence curves of the MITC3+ and MITC4 shell elements. Even though the distorted mesh is used, the MITC3+ shell element still shows good results unlike the MITC4 shell element.

3. CONCLUSIONS

We presented the performance of the MITC3+ triangular shell element recently developed in convergence studies. The results are compared with the MITC4 quadrilateral shell element, which has been widely used in finite element analysis of shells. The MITC3+ shell element showed the excellent behavior even when distorted meshes are used. In uniform meshes, the performance of the MITC3+ shell element is as good as that of the 4-node MITC4 shell element. In distorted meshes, the MITC3+ shell element presented much better performance than the MITC4 shell element in the bending-dominated shell problems. We expect that, due to its superior performance, the MITC3+ triangular shell element will be widely used in finite element analysis of shells.

REFERENCES

- Bathe K.J. (1996), "Finite element procedures", *Prentice Hall*, New York.
- Chapelle D., Bathe K.J. (2011), "The finite element analysis of shells – fundamentals, Second Edition", Springer-Verlag, Berlin.
- Hiller J.F., Bathe K.J. (2003) "Measuring convergence of mixed finite element discretizations: an application to shell structures", *Computers and Structures*, **81**, 639-654.
- Jeon, H.M., Lee Y., Lee P.S. and Bathe K.J. (2015), "The MITC3+ shell element in geometric nonlinear analysis", *Computers and Structures*, **146**, 91-104.
- Lee Y., Jeon, H.M. and Lee, P.S. and Bathe K.J. (2015), "The modal behavior of the MITC3+ triangular shell element", *Computers and Structures*, **153**, 148-164.
- Lee Y., Lee, P.S. and Bathe, K.J. (2014), "The MITC3+ shell finite element and its performance", *Computers and Structures*, **138**, 12-23.
- Lee Y., Yoon K., Lee P.S. (2012) "Improving the MITC3 shell finite element by using the Hellinger-Reissner principle", *Computers and Structures*, **110-111**, 93-106.
- Lee P.S., Noh H.C., Bathe K.J. (2007), "Insight into 3-node triangular shell finite elements : the effects of element isotropy and mesh patterns", *Computers and Structures*, **85**, 404-418.
- Lee, P.S., Bathe, K.J. (2004), "Development of MITC isotropic triangular shell finite elements", *Computers and Structures*, **82**, 945-962.
- Lee, P.S., Bathe, K.J. (2002), "On the asymptotic behavior of shell structures and the evaluation in finite element solutions", *Computers and Structures*, **80**, 235-255.